Analysis of the mKir2.1 channel activity in potassium influx defective *Saccharomyces cerevisiae* strains determined as changes in growth characteristics

Guido Hasenbrink[a], Sarah Schwarzer[a], Lucie Kolacna[b], Jost Ludwig[c], Hana Sychrova[b], Hella Lichtenberg-Fraté[a,*]

[a] *Molecular Bioenergetics, IZMB, Universität Bonn, Kirschallee 1, 53115 Bonn, Germany*
[b] *Department of Membrane Transport, Institute of Physiology, Academy of Sciences of the Czech Republic, Videnska 1083, 142 20 Prague 4, Czech Republic*
[c] *Physiologisch-chemisches Institut, Universität Tübingen, Hoppe-Seyler-Strasse 4, 72076 Tübingen, Germany*

Received 13 December 2004; revised 24 January 2005; accepted 4 February 2005

Available online 21 February 2005

Edited by Francesc Posas

Abstract **Potassium uptake defective *Saccharomyces cerevisiae* strains (Δ*trk1,2* and Δ*trk1,2* Δ*tok1*) were used for the phenotypic analysis of the mouse inward rectifying Kir2.1 channel by growth analysis. Functional expression of both, multi-copy plasmid and chromosomally expressed GFP-mKir2.1 fusion constructs complemented the potassium uptake deficient phenotype in a pH_{out} dependent manner. Upon application of Hygromycin B to chromosomally mKir2.1 expressing cells, significantly lower toxin sensitivity (EC_{50} 15.4 μM) compared to Δ*trk1,2* Δ*tok1* cells (EC_{50} 2.6 μM) was observed. Growth determination of mKir2.1 expressing strains upon application of Ag^+, Cs^+ and Ba^{2+} as known blockers of mKir2.1 channels revealed significantly decreased channel function. Cells with mKir2.1 were about double sensitive to $AgNO_3$, 350-fold more sensitive to CsCl and 1500-fold more sensitive to $BaCl_2$ in comparison to the respective controls indicating functional expression and correct pharmacology.**

Keywords: mKir2.1; Functional complementation; Growth characteristics; Phenotypic analysis; *Saccharomyces cerevisiae*

1. Introduction

Mammalian cells express a diverse array of transmembrane ion-channel proteins that selectively regulate the movement of ions across cellular membranes. With K^+ as the most abundant cellular cation, K^+ channels play pivotal roles in a number of essential processes like electrical activity of excitable cells, cellular K^+ homeostasis and, indirectly, pH regulation. Kir2.1 is a K^+ selective channel present in many excitable and non-excitable mammalian tissues [1], whose voltage-dependent high-affinity binding of intracellular blocking cations (spermine, spermidine, Mg^{2+}; [2–5]) underlies inward rectification. Kir2.1 subunits are believed to underlie the cardiac inward rectifying current I_{K1} that is considered to contribute significantly to the repolarising current during the terminal phase of the action potential (AP) and serves as the primary conductance controlling the resting potential in ventricular myocytes [6]. Mutations in the KCNJ2 gene that encodes Kir2.1 subunits are causative to the inherited Andersen syndrome (AS) long-QT disorder with ventricular arrhythmia and skeletal development abnormalities [7]. In view of the essential roles and great diversity of K^+ channels, the search for specific K^+ channel modulators for the targeted opening or closing of subtypes of channels has since long been prioritised to enable efficient therapeutic applications [8,9]. However, only few approaches [10,11] addressed expression of mammalian channels in yeast to serve as potential medium to high-throughput pre-screening system for pharmacological active compounds.

In the eukaryotic unicellular organism *Saccharomyces cerevisiae*, two closely related plasma membrane localised K^+ translocation systems, Trk1 and Trk2 mediate K^+ uptake to maintain a high intracellular potassium concentration to counterbalance the high negative charge on nucleic and amino acids. The third major K^+ translocation system, encoded by the *TOK1* gene, is a voltage-dependent outward rectifying K^+ channel [12] that under certain conditions also mediates inward K^+ uptake [13].

Previous studies reported functional expression of plant [14–16] and vertebrate inward rectifying K^+ channels [10,11] in *S. cerevisiae* Δ*trk1,2* double mutants. Both kinds of K^+ channels, though originating from different kingdoms are activated at hyperpolarised membrane voltages and mediate inward K^+ fluxes at membrane potentials more negative than the K^+ equilibrium potential (E_K). The increased K^+ requirement of the *S. cerevisiae* Δ*trk1,2* mutant is accompanied by the inability to grow on low pH medium [17] and high hyperpolarisation [18], thereby enabling functional expression of hyperpolarisation activated K^+ channels leading to the restoration of wild-type growth phenotype on low potassium media.

The objective of this study was to evaluate the yeast based test system as a diagnostic tool for mammalian K^+ selective channels by growth determination of functionally complemented K^+ uptake defective yeast strains. The mKir2.1 cDNA was expressed in *S. cerevisiae* strains carrying double or triple and combination of deletions of *trk1*, *trk2* and *tok1*. The results were indicative for the substitution of mKir2.1 for the endogenous yeast potassium uptake systems with regard to the potassium uptake deficient, low external pH sensitive and highly hyperpolarised phenotype. Known inhibitors of the mKir2.1 channel [11,19–21] strongly impaired the ability to

*Corresponding author. Fax: +49 228 73 55 04.
E-mail address: h.lichtenberg@uni-bonn.de (H. Lichtenberg-Fraté).

0014-5793/$30.00 © 2005 Published by Elsevier B.V. on behalf of the Federation of European Biochemical Societies.
doi:10.1016/j.febslet.2005.02.025

grow under limiting potassium conditions. The study provided evidence that yeast is a sensitive and practical model system for fast and reliable pharmacological pre-screening by utilising the advantages of growth determination in an unicellular eukaryotic organism because the response to pharmacological active compounds can be significant, the life cycle is short and yeast cells are easy to maintain.

2. Materials and methods

2.1. Yeast strains and growth conditions

Haploid *S. cerevisiae* yeast strains used throughout this study are listed in Table 1. Strains were grown aerobically at 30 °C. Nutritional requirements appropriate for selection and maintenance of mutants and plasmids in the transformed strains were scored on liquid complete synthetic SDAP medium [22] consisting of 0.5% D-glucose, vitamins, trace elements, amino acids and salts without uracil and leucine (for episomal expression of mKir2.1; the latter to utilise the LEU2-d function of the pYEX-BX vector to increase for plasmid copy numbers) or without leucine (for chromosomal expression of mKir2.1). The medium was adjusted to pH 5.9 with phosphoric acid and supplemented with the appropriate amount of KCl. All medium components were dissolved in ultrapure MilliQ water. Hygromycin B and the salts $BaCl_2$, CsCl and $AgNO_3$ were dissolved in MilliQ water and 3-bicyclo[2.2.1]hept-2-yl-benzene-1,2-diol (48F10, ChemBridge Corporation, San Diego, CA) in DMSO. $AgNO_3$ stock solutions were kept in the dark to avoid reduction of Ag^+ to Ag^0. $BaCl_2$ containing media were prepared without SO_4 salts. All amino acids were purchased from Fluka; DMSO and the metals salts were obtained from Sigma–Aldrich. All components were of analytical quality.

2.2. Plasmid construction

The applied episomal vector was the high copy *Escherichia coli*/yeast shuttle vector pYEX-BX (Clontech, Palo Alto, USA). A GFP-mKir2.1 plasmid (pYEGFP-C1-mKir2.1) was obtained from N. Klöcker (University of Freiburg). Plasmid pYEX-GFP-mKir2.1, used to express the yeast enhanced *yEGFP* of *Aequorea victoria* [23] mouse Kir2.1 fusion gene under the control of the *CUP1* promoter was obtained by standard DNA manipulations according to [24] and used to transform mutant yeast strains to uracil and leucine prototrophy by standard methods [25]. The applied integrating vectors were the p774 plasmid that targets integration to the genomic *LEU2* locus [26] and the p77x plasmid that targets integration to the *TOK1* locus. p77x was generated from p774 by replacing the *LEU2* targeting regions with ~400 bp of *TOK1* 5′ and 3′ non-coding sequence, respectively. In both gene replacement constructs, the expression of the GFP-mKir2.1 construct was under control of the *PMA1*-promoter. Following transformation and selection for leucine and uracil prototrophy the correct integrations were confirmed by PCR and Southern blot analysis. As an ER marker, a fusion comprising the signal sequence of the prepro-alpha-mating factor (sig) [27], the monomeric *red fluorescent protein* mRFP [28] and the 'HDEL' ER-retention signal [29] was generated in a modified p77x to yield strain PLY240-sig/mRFP/HDEL (*tok1*::P_{PMA1}-sig/mRFP/HDEL).

2.3. Cellular potassium content

Cells were grown in SDAP media supplemented with 10 or 50 mM KCl and adjusted to pH_{out} 5.9 or 6.5 to late stationary phase (20 h) and collected on Millipore membrane filters (pore size 0.2 μm). Following rapid washing with a 20 mM $MgCl_2$ solution, the cells were acid-extracted with 10 mM $MgCl_2$ and 0.2 M HCl overnight at room temperature. The potassium content was analysed in supernatants by atomic absorption spectroscopy (Shimadzu AA-660). All measurements were repeated at least four times.

2.4. Fluorescence microscopy

Microscopic images were obtained with a ZEISS Axioplan microscope with ZEISS Plan Neofluar 100× objective. The excitation source was a 50 W Hg vapour arc lamp. The *gfp* fluorescence was visualised by a 450–490 nm band pass (BP) excitation filter and an 515–565 nm BP emission filter. Images were taken by a CCD camera (CF8/1 DXC, Kappa).

2.5. Immuno-blotting

Yeast cells were grown to an OD of ~1 (corresponding to 1.2×10^7 cells/ml). 10 ml of cells were harvested by centrifugation and washed with distilled water. Protein extraction was carried out using the alkaline lysis method [30]. Protein content was determined using the Bio-Rad protein assay (Bio-rad Laboratories). For detection of GFP and GFP/Kir2.1 fusion proteins ~20 μg of total protein were separated by SDS–PAGE (10% polyacrylamide) and transferred to nitrocellulose membranes (Amersham) by wet blotting. Blots were incubated with an anti-GFP antibody (mixture of two monoclonal antibodies, Roche) and after incubation with a secondary alkaline phosphatase-conjugated goat anti-mouse antibody (IgG, Sigma–Aldrich) labelled proteins were detected using BCIP/NBT (Sigma–Aldrich).

Table 1
Yeast strains

Strain	Genotype	References
PLY232	*MATa his3-Δ200 leu2-3,112 trp1-Δ901 ura3-52 suc2-Δ9*	Bertl et al. [17]
PLY238	*MATa his3-Δ200 leu2-3,112 trp1-Δ901 ura3-52 suc2-Δ9 tok1Δ1::HIS3*	Bertl et al. [17]
PLY240	*MATa his3-Δ200 leu2-3,112 trp1-Δ901 ura3-52 suc2-Δ9 trk1Δ51 trk2Δ50::kanMX*	Bertl et al. [17]
PLY246	*MATa his3-Δ200 leu2-3,112 trp1-Δ901 ura3-52 suc2-Δ9 trk1Δ51 trk2Δ50::kanMX tok1Δ1::HIS3*	Bertl et al. [17]
PLY240T-GFP-mKir2.1	*MATa his3-Δ200 leu2-3,112 trp1-Δ901 ura3-52 suc2-Δ9 trk1Δ51 trk2Δ50::kanMX tok1::P_{PMA1}-GFP-mKir2.1*	This study
PLY240T-GFP	*MATa his3-Δ200 leu2-3,112 trp1-Δ901 ura3-52 suc2-Δ9 trk1Δ51 trk2Δ50::kanMX tok1::P_{PMA1}-GFP*	This study
PLY240L-GFP-mKir2.1	*MATa his3-Δ200 leu2-3,112 trp1-Δ901 ura3-52 suc2-Δ9 trk1Δ51 trk2Δ50::kanMX leu2::P_{PMA1}-gfp-mKir2.1*	This study
PLY240L-GFP	*MATa his3-Δ200 leu2-3,112 trp1-Δ901 ura3-52 suc2-Δ9 trk1Δ51 trk2Δ50::kanMX leu2::P_{PMA1}-gfp*	This study
PLY246L-GFP	*MATa his3-Δ200 leu2-3,112 trp1-Δ901 ura3-52 suc2-Δ9 trk1Δ51 trk2Δ50::kanMX tok1Δ1::HIS3 leu2::P_{PMA1}-gfp*	This study
PLY240-sig/mRFP/HDEL	*MATa his3-Δ200 leu2-3,112 trp1-Δ901 ura3-52 suc2-Δ9 trk1Δ51 trk2Δ50::kanMX tok1::P_{PMA1}-sig/mRFP/HDEL*	This study
PLY240 [pYEX-GFP-mKir2.1]		This study
PLY240 [pYEX-GFP]		This study
PLY246 [pYEX-GFP-mKir2.1]		This study
PLY240 [pYEX-GFP-TRK1]		This study
PLY240 [pYEX-GFP-TRK2]		This study

2.6. Assay conditions

For liquid growth determination, the minimal SDAP medium was chosen to precisely control KCl contents since YNB medium contains ~10 mM potassium (determined by Atomic absorption spectroscopy) which can confound attempts to monitor potassium dependent growth phenotypes. For quantitative assessment of growth phenotypes, cells were grown under permissive conditions (100 mM KCl) to the stationary phase, washed with MilliQ water and diluted in fresh medium to a start OD_{600} of 0.2 (pathlength 1 cm, Pharmacia Ultrospec 2000 Spectrophotometer) corresponding to 3×10^6 cells/ml. The growth was estimated by photometric determination of the turbidity at 600 nm in 15 min intervals in transparent 96-well microtitre plates using a microplate reader (Tecan, Spectrofluor Plus) with 30 °C incubation and constant agitation for 15 h. The growth of mKir2.1 expressing strains and corresponding controls were compared in 100 and 10 mM KCl at different concentrations of Hygromycin B, $AgNO_3$, CsCl, $BaCl_2$ and 3-bicyclo[2.2.1]hept-2-yl-benzene-1,2-diol. For each tested condition, at least four replicate tests were carried out on different days. Each experiment consisted of one control and up to nine test concentrations of the substances with inhibition scored between >0% and <100%. Tests were considered as valid when the turbidity of the control cultures increased at least fivefold during the incubation period.

2.7. Data capture and evaluation

Growth calculation was performed by the approximation of the area (A) under the growth curves obtained within 12.5 h incubation by the following equation:

$$A = \sum_{i=1}^{m-1} \left[\left(\frac{1}{2} (\mathrm{OD}_i + \mathrm{OD}_{i+1}) - \mathrm{OD}_1 \right) \cdot (t_{i+1} - t_i) \right]$$

where OD_i is the measured optical density; $i = 1$ to m is the number of measurements during the test time (12.5 h). Inhibitory effects were calculated by quantifying the extent of growth inhibition in the test cultures in comparison to control cultures. Corresponding EC_{50} values were determined by either Hill plot analysis for monophasic inhibition kinetics or by fitting biphasic kinetic curves according to:

$$G = G_{\mathrm{start}} \cdot \left[1 - \left((1 - E_1) \cdot \frac{c^n}{K_1 + c^n} \right) \right] \cdot \left[1 - \left((1 - E_2) \cdot \frac{c^m}{K_2 + c^m} \right) \right]$$

where c is the actual test substance concentration, G is the growth at concentration c, G_{start} the growth of the negative control culture (without test substance), $E_{1,2}$ the growth at maximum response relative to the negative culture control, $K_{1,2}$ are the half-saturation constants and n and m, respectively, are the indicators for the cooperativeness of the respective effect.

3. Results

Different *S. cerevisiae* uptake and efflux deficient yeast strains were used as hosts for the heterologous expression of the mouse inward rectifier Kir2.1 channel. The expression deployed two different strategies, the integration into the single *LEU2* and *TOK1* genomic loci whereby the K^+ channel cDNA was set under control of the constitutive *PMA1* promoter and the episomal expression using the pYEX-BX multicopy vector with *CUP1* promoter. Growth characteristics were observed by measuring the optical density in liquid SDAP media for 12.5 h. Liquid culture growth modulations were determined by calculation of a defined area (approximating the integral) under the individual OD_{600} growth-curves (Fig. 1A). Thereby, possible strain specific and compound induced altered growth characteristics like delayed lag-phase, different slopes of log-phase and corresponding entering of the plateau phase with variations of maximum cell density in the stationary phase (Fig. 1B) were taken into account.

In Fig. 2, the growth characteristics of different mKir2.1 expressing strains in SDAP media supplemented with 10 or 100 mM KCl are summarised. In comparison to the respective control strains that expressed the GFP gene either chromosomally or episomally and thus represented the Δ*trk1,2* or Δ*trk1,2* Δ*tok1* mutants, the GFP-mKir2.1 expressing strains exhibited clear growth advantages under limiting potassium (10 mM KCl) concentrations. The functional complementation of the yeast mutant phenotypes by mKir2.1 almost restored wild-type growth properties whereby differences in the growth complementation capability were dependent on the expression construct and level (Fig. 2, [31]). Except the Δ*trk1,2* mutant with *LEU2* locus integrated fusion construct, all GFP-mKir2.1 expressing strains exhibited enhanced growth on 10 mM KCl compared to that on 100 mM KCl. A similar phenotype was obtained by episomal expression of the endogenous *TRK1* or *TRK2* genes.

Another reported phenotype of Δ*trk1,2* and Δ*trk1,2* Δ*tok1* mutants is the sensitivity towards acidic external pH values particularly in combination with limited potassium. Grown in media containing external potassium concentrations

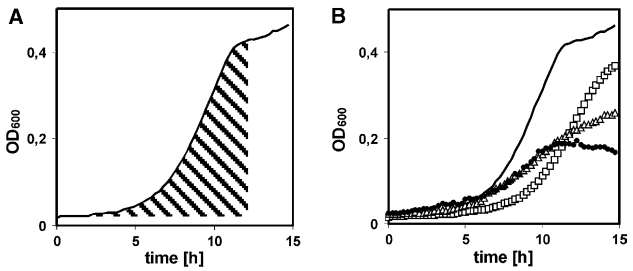

Fig. 1. (A) Growth characteristics were determined by calculation (approximative integral) of a defined area under the obtained OD_{600} curves within a time interval of 12.5 h (hatched area) to account for qualitative different growth curves as given in (B). In response to inhibitory substances growth curves were altered in different manners by 8 μM $AgNO_3$ (□), 100 μM $BaCl_2$ (△) and 8 μM 3-bicyclo[2.2.1]hept-2-yl-benzene-1,2-diol (●) compared to the control (—).

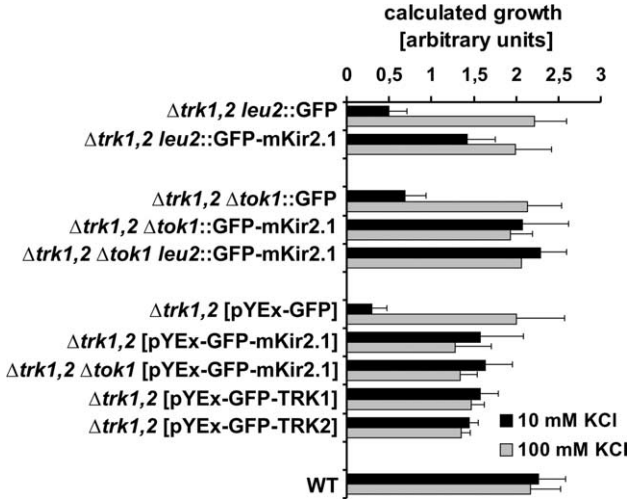

Fig. 2. The expression of mKir2.1 constructs functionally complemented the Δ*trk1,2* and Δ*trk1,2* Δ*tok1* mutant phenotype in 10 mM potassium. In comparison to the respective control strains that expressed the GFP gene either chromosomally or episomally the GFP-mKir2.1 expressing strains exhibited similar growth characteristics as the wild type (WT) or the endogenous TRK-transporters (*TRK1*, *TRK2*).

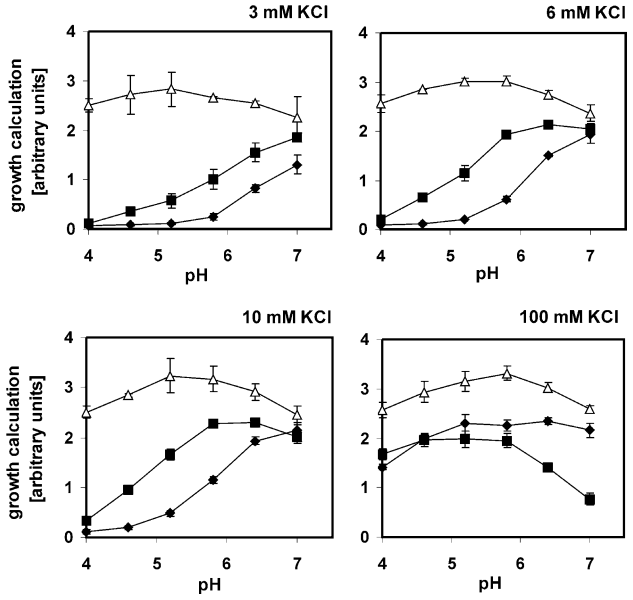

Fig. 3. pH_{out} dependency of mKir2.1 mediated growth under permissive (100 mM) and limiting potassium KCl concentrations. The Δ*trk1,2 tok1::*GFP-mKir2.1 (■) was compared to both, the respective control (Δ*trk1,2 tok1::GFP*) without mKir2.1 (◆) and the wt strain (△).

between 3 and 100 mM KCl and ranging from pH 4 to pH 7, the GFP-mKir2.1 expressing triple mutant showed a significant growth advantage at 3 mM KCl pH_{out} 5.9 or 6.5 and even at pH 7 (Fig. 3). The most remarkable growth advantages of the GFP-mKir2.1 expressing strain compared to the mutant were observed at 6 and 10 mM KCl, pH 5.9. That observation was also reflected by the cellular potassium content analysis revealing similar K^+_{int} concentrations at limiting (10 mM KCl) potassium concentrations in wild type and mKir2.1 expressing cells at pH 5.9, whereas the Δ*trk1,2* Δ*tok1* mutant cells contained significantly less intracellular potassium (Fig. 4). In 50 mM KCl, pH_{out} 5.9, a condition in which the growth

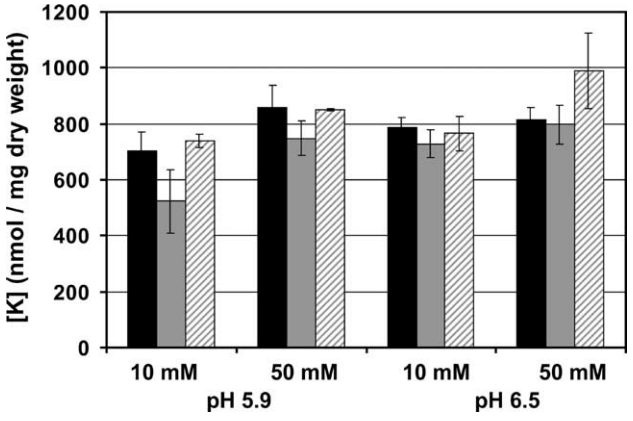

Fig. 4. Cellular potassium content of the wild type (black filled columns), the Δ*trk1,2* Δ*tok1* triple mutant (grey filled columns) and the GFP-mKir2.1 expressing triple mutant (hatched columns) in limiting (10 mM) and permissive (50 mM) KCl at different external pH values. Error bars represent S.E.M.

differences between the triple mutant and the mKir2.1 expressing strains were marginal, the intracellular potassium content almost approximated among the tested strains. Similar data were also obtained for the Δ*trk1,2* mutant and the *LEU2* locus GFP-mKir2.1 expressing strain (data not shown). At 50 mM KCl, pH_{out} 6.5 the mKir2.1 expressing triple mutant exhibited a distinct higher K^+_{int} content than either the wild type or the triple mutant.

The subcellular localisation of integrated or multi-copy gfp tagged mKir2.1 was investigated in *S. cerevisiae* Δ*trk1,2* Δ*tok1* cells (Fig. 5A, B and E) in comparison to the episomally expressed endogenous potassium transporters Trk1 or Trk2 (Fig. 5C and D). Microscopic inspection of the chromosomally expressed *GFP* revealed an evenly cytosolic distributed fluorescence whereas discrete punctiform labelling predominantly near or at the plasma membrane and around the nucleus was observed with GFP-mKir2.1 (Fig. 5A). The gfp fluorescence intensity was significantly enhanced by multi-copy expression (Fig. 5B–E). The reintroduced native plasma membrane transporters exhibited bright uniform ring-shape fluorescence near or at the plasma membrane (Fig. 5C and D) with GFP-Trk1 also accumulating around the nucleus similar to GFP-mKir2.1 (B, confirmed by DNA H33342 stain). Co-localisation of episomally expressed GFP-mKir2.1 with the ER marker sig/mRFP/HDEL revealed substantial overlay with the GFP-mKir2.1 mediated fluorescence (Fig. 5E). These observations indicated that at least partial incorporation of the heterologous channel into the plasma membrane is sufficient to account for the functional complementation of uptake deficient yeast mutants. Immunoblot analysis of GFP-mKir2.1 expressing strains with an anti-gfp antibody revealed in the majority of the strains the full length GFP-mKir2.1 product of 75 kDa (Fig. 6).

The sensitivity to Hygromycin B is known as reliable indicator of membrane potential. The knock out of both Trk transporters has been reported to result in considerable membrane hyperpolarisation [18]. The high sensitivity towards the positively charged toxin was used as indirect indicator of plasma membrane hyperpolarisation of the Δ*trk1,2* Δ*tok1* triple mutant in comparison to the mKir2.1 and *TRK1,2* expressing strain (Fig. 7). Under limiting potassium conditions (20 mM KCl) the triple mutant exhibited an extremely high sensitivity with an EC_{50} of 2.6 μM. Significantly lower sensitivity was observed in the chromosomally mKir2.1 expressing strain with an EC_{50} of 15.4 μM compared to the endogenous Trk1,2 mediated EC_{50} of 59.7 μM. Thus, the presence of the heterologous channel decreased the membrane potential and accordingly the sensitivity to Hygromycin B. This effect was not observed under permissive conditions (data not shown).

Various mono- and divalent cations such as Ag^+, Ba^{++} and Cs^+ [19–21] have been shown to block the mKir2.1 inward rectifying channel by different mechanisms. The effects of these cations on mKir2.1 in *S. cerevisiae* were tested by growth determination (Fig. 8). Application of all inhibitors produced biphasic growth inhibition kinetics, where the mKir2.1 specific inhibition preceded the residual growth inhibition of the parental mutants. Such inhibition kinetic was evaluated by the equation given in Section 2 to separate the effects. In the presence of increasing concentrations of CsCl, growth mediated by integrated GFP-mKir2.1 in the triple mutant was severely inhibited with an EC_{50} of 70 μM compared to the respective control with an EC_{50} of 24.4 mM (Fig. 8A).

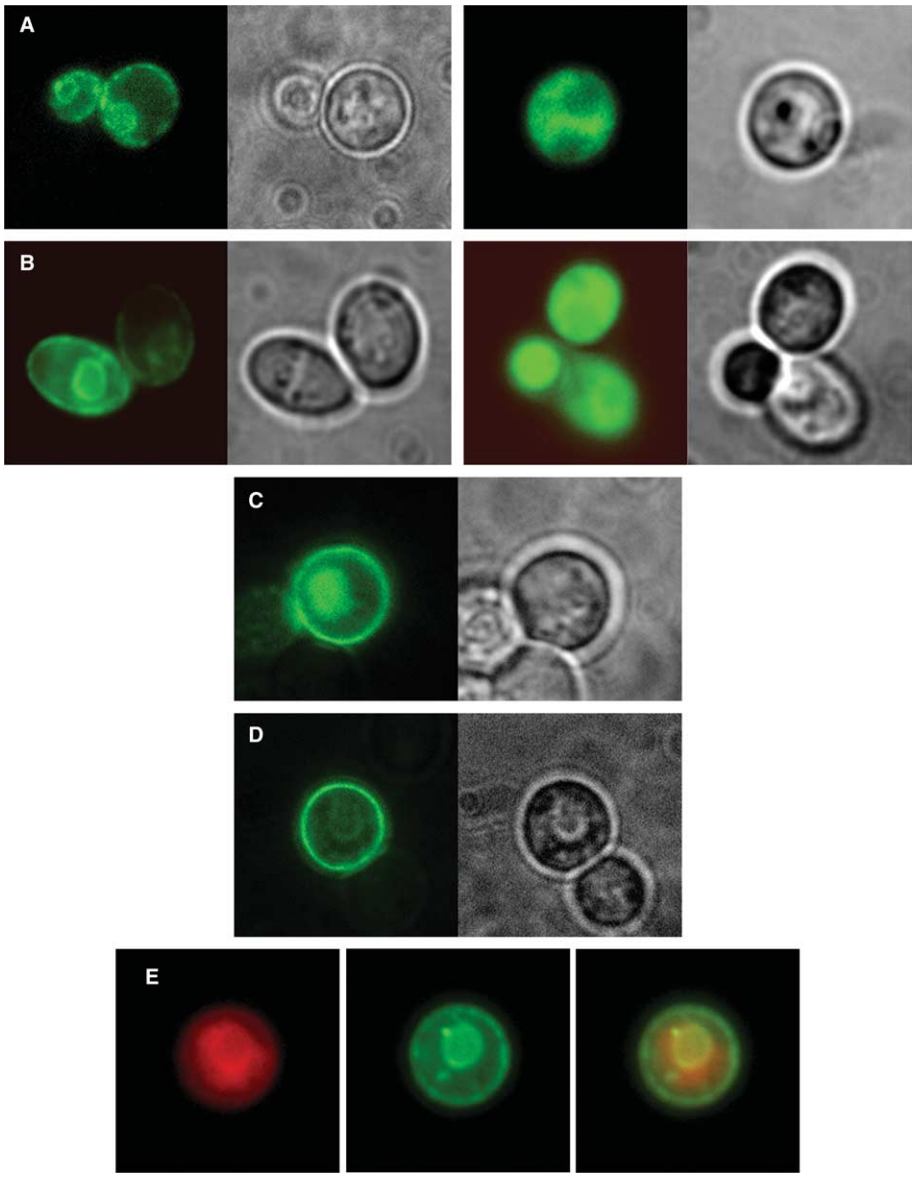

Fig. 5. Subcellular localisation of gfp-tagged mKir2.1 compared to gfp-tagged endogenous Trk1 and Trk2 and corresponding control (only GFP). (A) *S. cerevisiae* Δ*trk1,2 tok1::*GFP-mKir2.1 with punctiform fluorescence label near or at the plasma membrane and around the nuclear envelope (left panel) and Δ*trk1,2 tok1::GFP* with even cytosolic fluorescence distribution (right panel). (B) Δ*trk1,2* Δ*tok1* multi-copy plasmid GFP-mKir2.1 expression (left panel) with ring-shape fluorescence (plasma membrane and nuclear envelope) and corresponding control (right panel), in both cases with enhanced intensity compared to (A). Δ*trk1,2* Δ*tok1* cells with multi-copy plasmid GFP-*TRK1* (C), or GFP-*TRK2*, (D) expression. (E) sig/mRFP/HDEL (left panel), Δ*trk1,2* Δ*tok1* with multi-copy plasmid GFP-mKir2.1 (middle panel) and overlay image (right panel) indicative for mKir2.1 plasma membrane localisation.

Multi-copy mKir2.1 expressing Δ*trk1,2* cells were inhibited with an EC_{50} value of 370 μM compared to cells episomally expressing either *TRK1* (EC_{50} of 17.8 mM) or *TRK2* (EC_{50} of 19.5 mM, Fig. 8B). Under permissive conditions (100 mM KCl), this inhibitory effect was not obtained (data not shown). Thus, Cs cations specifically inhibited mKir2.1 mediated growth. Silver was applied as $AgNO_3$ and shown to specifically inhibit growth of the mKir2.1 expressing strains with an EC_{50} of 0.57 and 0.52 μM in Δ*trk1,2* or Δ*trk1,2* Δ*tok1* cells, respectively (Fig. 8C). The parental mutants revealed EC_{50} values of 1.17 and 1.64 μM. Barium was supplied as $BaCl_2$ to the growth media and in the presence of increasing concentrations shown to inhibit mKir2.1 mediated growth with an EC_{50} of 2.3 μM compared to the respective control with an EC_{50} value of 3.6 mM (Fig. 8D).

Recently, the compound 3-bicyclo[2.2.1]hept-2-yl-benzene-1,2-diol was identified as specific inhibitor of Kir2.1 and Kv2.1 channels with EC_{50} values of 60 and 1 μM, respectively, determined by patch-clamp experiments [11]. Evaluation of the current yeast growth based assay, that is potassium content defined minimal medium and usage of the triple Δ*trk1,2* Δ*tok1* mutant chromosomally expressing GFP-mKir2.1 with this compound revealed an growth inhibition EC_{50} value of 5.1 μM compared to the respective control (EC_{50} of 28.4 μM) under limiting potassium conditions (Fig. 9). At 100 mM KCl for both, the GFP-mKir2.1 expressing and the

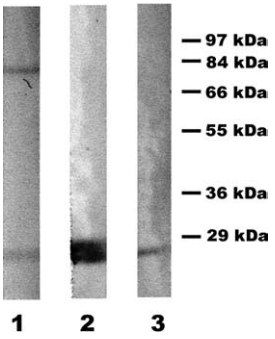

Fig. 6. Immunoblot analysis of protein extracts obtained from the mKir2.1 expressing strain Δ*trk1,2 tok1::*GFP-mKir2.1 (lane 1), the control Δ*trk1,2* [pYEX-GFP] (lane 2) and the mutant Δ*trk1,2* (lane 3) with an anti-GFP antibody. The ~75 kDa band corresponds to the size of the gfp-mKir2.1 fusion protein. Below the 29 kDa marker band a signal corresponding to unspecific cross reaction was detected.

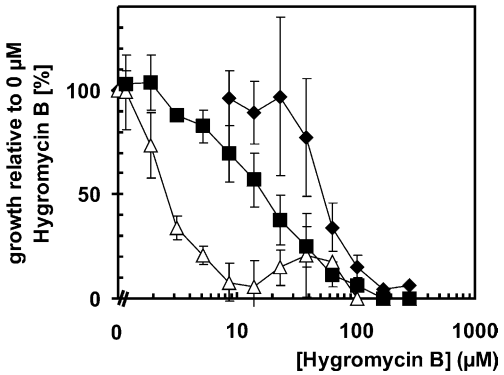

Fig. 7. Growth effects of Hygromycin B under non-permissive (20 mM KCl) conditions: Control Δ*trk1,2 tok1::GFP* cells (△), the mKir2.1 expressing strain Δ*trk1,2 tok1::*GFP-mKir2.1 (■) and *TRK1,2* Δ*tok1* (◆) cells were grown in the presence of increasing Hygromycin B concentrations. Calculated EC_{50} values are 2.6, 15.4 and 59.7 µM, respectively.

control strain, clear cytotoxic effects could be observed with EC_{50} values of 46.3 and 22.5 µM (data not shown).

4. Discussion

We investigated *S. cerevisiae* potassium uptake defective strains transformed with integrative or episomal mKir2.1 and GFP-mKir2.1 plasmids to identify and characterise the channel activity through an assay based on changes in growth characteristics. Since the yeast mutants exhibit clearly defined growth phenotypes the indicator strains expressing the functional mKir2.1 enable quantification of both the activation and inactivation function of the channel. Investigations comprised both specificity and sensitivity of the system. The determination of growth characteristics changes as approximation of the integral under the measured growth curve of the specific culture in wells of the microtiter plate served sufficient to account for several different effects like delayed growth phase,

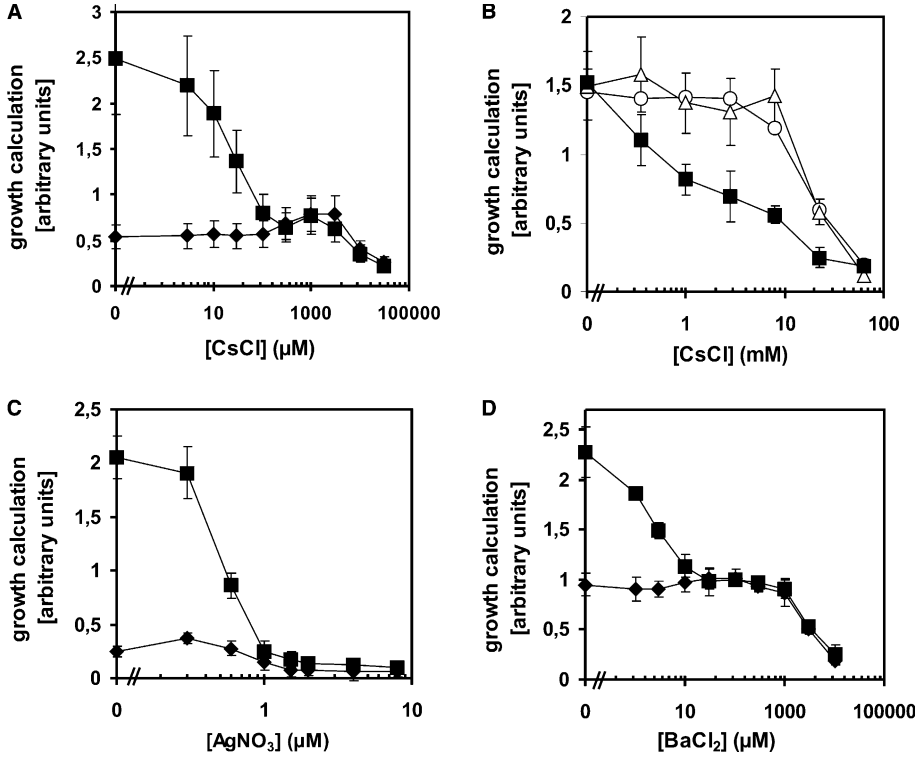

Fig. 8. The growth mediated by chromosomal expression of mKir2.1 at 10 mM KCl in the Δ*trk1,2* Δ*tok1* mutant (■) was specifically blocked by CsCl (A) (EC_{50} value of 70 ± 18 µM), $AgNO_3$ (EC_{50} value of 0.52 ± 0.11 µM) (C), and $BaCl_2$ (EC_{50} value of 2.32 ± 0.53 µM) (D). In each case the corresponding control strain without mKir2.1 (◆) indicated cytotoxic effects. (B) Growth mediated by multi-copy plasmid expression of mKir2.1 at 10 mM KCl in the double Δ*trk1,2* mutant (■) was shown to be significantly more sensitive to CsCl (EC_{50} = 0.37 mM) compared to that mediated by multi-copy expression of endogenous *TRK1* (△) or *TRK2* (○) with EC_{50} values of 17.8 and 19.5 mM, respectively.

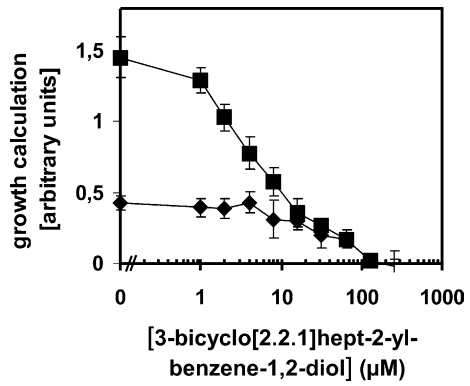

Fig. 9. Growth inhibition of Δ*trk1,2 tok1::*GFP-mKir2.1 cells (■) in the presence of increasing concentrations of 3-bicyclo[2.2.1]hept-2-yl-benzene-1,2-diol and limited potassium (10 mM KCl). The mKir2.1 mediated growth was specifically inhibited with an EC_{50} of 5.1 ± 1.5 μM. The corresponding control (Δ*trk1,2 tok1::GFP*, (◆)) revealed also strong cytotoxic effects with an EC_{50} of 28.4 ± 5.9 μM.

flat or steep logarithmic phase and early or late entering of the stationary phase (Fig. 1A and B).

4.1. Specificity

The mKir2.1 channel functionally complemented the uptake deficient phenotype in Δ*trk1,2* or Δ*trk1,2* Δ*tok1* cells regardless of integrative or episomal expression and in cells lacking both potassium uptake and efflux transport systems (Δ*trk1* Δ*trk2* Δ*ena1–4* Δ*nha1*) cells (Fig. 2, [31,32]). Nevertheless, remarkable differences of growth were noticed upon different levels of expression, a phenomenon also observed in mKir2.1 expressing alkali-metal-cation efflux defective strains, where the level of mKir2.1 protein expression influenced the sensitivity of cell to external KCl [32]. For instance, under permissive conditions (100 mM KCl) episomal expression of mKir2.1 slightly impaired growth of the strains in comparison to that in limited potassium concentrations. This phenotype was dependent on the expression of a functional channel since mutant GFP-mKir2.1 cDNAs (R67W, D71V, data not shown) did not impair growth in 100 mM KCl.

As mammalian channel, the mKir2.1 inward rectifier is adapted to a nearly neutral physiological environment. This is in contrast to the usual optimal growth pH of yeast cultures of around pH 5. Our investigations revealed not only that the functionally expressed mKir2.1 also complemented the reported pH_{out} sensitive Δ*trk1,2* mutant phenotype [17], but that a significant growth advantage could still be observed at pH_{out} 7 at very low external potassium concentrations (3 mM, Fig. 3). Thus, the mKir2.1 activity covers in this genetic background two pH_{out} units, an observation that is similar to results obtained in alkali-metal-cation efflux defective cells (Δ*ena1–4* Δ*nha1*) where mKir2.1 channel mediated pH_{out}-dependent increased sensitivity to external KCl [32]. The lowest tested concentration (3 mM KCl) appeared different from related approaches using 0.1 or 2 mM external KCl [33,11]. However, [11] involved YNB as medium basis that contains ~10 mM endogenous contaminant potassium (determined by Atomic absorption spectroscopy). By using the synthetic minimal SDAP medium potassium concentrations can be more accurately controlled.

Under limiting potassium concentrations (10 mM KCl) at pH 5.9 triple mutant cells had a decreased potassium concentration compared to wild-type cells (Fig. 4). The expression of mKir2.1 in the triple mutant is in such conditions accompanied by an increase in cellular potassium content to the level of wild-type cells. Under limiting potassium concentrations at pH 6.5 as well as permissive conditions (50 mM KCl) at pH 5.9, the intracellular potassium content of the investigated strains approximated. However, in mKir2.1 expressing cells grown in 50 mM KCl, pH 6.5 the cellular potassium concentration was increased compared to both wild type and triple mutant cells. The observed growth inhibition of the mKir2.1 expressing strain at 100 mM KCl, pH_{out} 6.5 and 7 (Fig. 3) together with the high K^+_{int} concentration at 50 mM KCl pH_{out} 6.5 (Fig. 4) suggests that the channel activity under these conditions caused an increased membrane permeability for K^+ and thus a growth inhibiting depolarisation that is not apparent in the triple mutant, where K^+ is mainly translocated by unspecific mechanisms [34–36]. The potassium homeostasis appears pH_{out} dependent connected to a rather limited cellular content range between ~600 and ~900 nmol/mg dry weight whereby both, decreased (Δ*trk1,2* and Δ*trk1,2* Δ*tok1*) and exceeding (*tok1*::GFP-mKir2.1) K^+_{int} concentrations are involved in the observed suboptimal growth phenotypes.

In *S. cerevisiae*, the endoplasmatic reticulum (ER) centres not only around the nucleus but is attached or at least close to the plasma membrane [37]. In addition, yeast strains episomally expressing different genes have been shown to accumulate large amounts of the heterologous membrane protein by ER membrane proliferation [38,39]. We thus investigated the subcellular localisation of chromosomally and multi-copy expressed GFP-mKir2.1 in comparison to multi-copy expressed GFP-*TRK1* and GFP-*TRK2* (Fig. 5). In Δ*trk1,2* Δ*tok1* cells GFP-mKir2.1 protein localised around the nucleus (confirmed by H33342 DNA stain) and close to or at the plasma membrane in primarily punctiform (chromosomal) or evenly ring-shape (episomal) patterns. Additional internal fluorescence was among the endogenous Trk transporters only visible for GFP-Trk1, probably due to the plasmid bound overexpression. Co-localisation with an ER restrained prepro-alpha-factor-rfp fusion (sig/mRFP/HDEL) revealed a significant overlap of the two fluorophores indicative of partial retention of the GFP-mKir2.1 fusion construct in the ER. Accumulation of aberrant ER proliferation and overexpression induced proteotoxicity was not detected and the obtained functional data suggest that the (even low) protein amount correctly targeted to the plasma membrane is necessary and sufficient to complement the mutant phenotypes. This was also demonstrated by the addition of the positively charged toxin Hygromycin B (Fig. 7). The antibiotic was massively taken up by hyperpolarised cells (EC_{50} of 2.6 μM in Δ*trk1,2* Δ*tok1* versus 59.7 μM in *TRK1,2* cells) and inhibited intracellularly protein synthesis and thus growth. The observed reduced intoxination by Hygromycin B in mKir2.1 expressing cells (EC_{50} 15.4 μM) indicated a distinct less hyperpolarised membrane depended on K^+ translocation. Comparable to results obtained for plant CNGC channels [40] our observations suggested that cells encounter the channel activity also for proper maintenance of the membrane potential. In summary, these results provided evidence that in strains with stably integrated or episomally expressed mKir2.1 the channel is functional.

4.2. Sensitivity

The sensitivity of mKir2.1 in the yeast microenvironment was investigated by exposure to known blockers of the channel. Among CsCl, $AgNO_3$ and $BaCl_2$, cesium (Fig. 8A and B) exerted the strongest channel specific effect by an EC_{50} of 70 μM versus 24.4 mM in chromosomally expressing cells and 370 μM versus 17.8 or 19.5 mM in episomally expressing mKir2.1, *TRK1* or *TRK2*, respectively cells. Cs^+ was shown to block Kir2.1 channels and comparable inhibition parameters of $K_D = 101 \pm 7$ μM at −97 mV were determined in patch-clamp experiments [21]. Silver exposure yielded the lowest nominal EC_{50} values (0.57 and 0.52 μM, Fig. 8C) but caused also a significant cytotoxic effect because the calculated EC_{50} values of 1.17 and 1.64 μM for Δ*trk1,2* and Δ*trk1,2* Δ*tok1* cells, respectively, were in the same order of magnitude as for the wild type (EC_{50} of 2.6 μM, data not shown). A complete block of mKir2.1 mediated currents was observed upon 0.2 μM $AgNO_3$ application in patch-clamp experiments [19], the yeast based mKir2.1 growth determination data are thus within the same order of magnitude. $BaCl_2$ inhibited mKir2.1 protein mediated growth with an EC_{50} of 2.3 μM (Fig. 8D) that is significantly less than the reported IC_{50} of 16.2 ± 3.4 μM of homomeric Kir2.1 channels in *Xenopus* oocytes but similar to that of native I(K1) 4.7 ± 0.5 μM Ba^{++} sensitivities [20]. The compound 3-bicyclo[2.2.1]hept-2-yl-benzene-1,2-diol was identified as specific inhibitor of Kir2.1 channels in a primary yeast screen with an EC_{50} value of 60 μM determined by patch-clamp experiments [11]. The specific mKir2.1 effect of this compound could be confirmed in the current assay (Fig. 9) by an EC_{50} value of 5.1 μM in comparison to Trk1 and Trk2 (EC_{50} of 6.9 and 27.4 μM, respectively; data not shown) for which a K^+ channel related topology was proposed [41]. In addition, severe cytotoxic effects were detected under limiting (EC_{50} of 28.4 μM) and permissive (EC_{50} of 22.5 μM) potassium concentrations.

4.3. Summary

Most proteins are sufficiently complex to necessitate their production in living systems, mostly by recombinant DNA technology. As such, the choice of recombinant yeast expression hosts particularly for mammalian K channels may provide advantages for primary pharmacological or toxicological screening. The method of growth change determination is reliable to qualitatively measure specific effects. The method is also suited to quantitatively characterise heterologously expressed mKir2.1 inward rectifying channels by toxicological parameters like effective concentrations (EC) of potential inhibitors.

Acknowledgements: This work was supported by EC grant QLK3-CT2001-00401. The authors thank B. Kirberg for excellent technical assistance.

References

[1] Raab-Graham, K.F., Radeke, C.M. and Vandenberg, C.A. (1994) Molecular cloning and expression of a human heart inward rectifier potassium channel. Neuroreport 5, 2501–2505.
[2] Stanfield, P.R., Davies, N.W., Shelton, P.A., Sutcliffe, M.J., Khan, I.A., Brammar, W.J. and Conley, E.C. (1994) A single aspartate residue is involved in both intrinsic gating and blockage by Mg^{2+} of the inward rectifier, IRK1. J. Physiol. 478, 1–6.
[3] Lopatin, A.N., Makhina, E.N. and Nichols, C.G. (1994) Potassium channel block by cytoplasmic polyamines as the mechanism of intrinsic rectification. Nature 372, 366–369.
[4] Fakler, B., Brandle, U., Glowatzki, E., Weidemann, S., Zenner, H.P. and Ruppersberg, J.P. (1995) Strong voltage-dependent inward rectification of inward rectifier K^+ channels is caused by intracellular spermine. Cell 80, 149–154.
[5] Yang, J., Jan, Y.N. and Jan, L.Y. (1995) Control of rectification and permeation by residues in two distinct domains in an inward rectifier K^+ channel. Neuron 14, 1047–1054.
[6] Miake, J., Marban, E. and Nuss, H.B. (2003) Functional role of inward rectifier current in heart probed by Kir2.1 overexpression and dominant-negative suppression. J. Clin. Invest. 111, 1529–1536.
[7] Tristani-Firouzi, M., Jensen, J.L., Donaldson, M.R., Sansone, V., Meola, G., Hahn, A., Bendahhou, S., Kwiecinski, H., Fidzianska, A., Plaster, N., Fu, Y.H., Ptacek, L.J. and Tawil, R. (2002) Functional and clinical characterization of KCNJ2 mutations associated with LQT7 (Andersen syndrome). J. Clin. Invest. 110, 381–388.
[8] Miura, T. and Miki, T. (2003) ATP-sensitive K^+ channel openers: old drugs with new clinical benefits for the heart. Curr. Vasc. Pharmacol. 1, 251–258.
[9] Boy, K.M., Guernon, J.M., Sit, S.Y., Xie, K., Hewawasam, P., Boissard, C.G., Dworetzky, S.I., Natale, J., Gribkoff, V.K., Lodge, N. and Starrett Jr., J.E. (2004) 3-Thio-quinolinone maxi-K openers for the treatment of erectile dysfunction. Bioorg. Med. Chem. Lett. 14, 5089–5093.
[10] Tang, W., Ruknudin, A., Yang, W.P., Shaw, S.Y., Knickerbocker, A. and Kurtz, S. (1995) Functional expression of a vertebrate inwardly rectifying K^+ channel in yeast. Mol. Biol. Cell. 6, 1231–1240.
[11] Zaks-Makhina, E., Kim, Y., Aizenman, E. and Levitan, E.S. (2004) Novel neuroprotective K^+ channel inhibitor identified by high-throughput screening in yeast. Mol. Pharmacol. 65, 214–219.
[12] Ketchum, K.A., Joiner, W.J., Sellers, A.J., Kaczmarek, L.K. and Goldstein, S.A. (1995) A new family of outwardly rectifying potassium channel proteins with two pore domains in tandem. Nature 376, 690–695.
[13] Fairman, C., Zhou, X. and Kung, C. (1999) Potassium uptake through the TOK1 K^+ channel in the budding yeast. J. Membr. Biol. 168, 149–157.
[14] Anderson, J.A., Nakamura, R.L. and Gaber, R.F. (1994) Heterologous expression of K^+ channels in *Saccharomyces cerevisiae*: strategies for molecular analysis of structure and function. Symp. Soc. Exp. Biol. 48, 85–97.
[15] Sentenac, H., Bonneaud, N., Minet, M., Lacroute, F., Salmon, J.M., Gaymard, F. and Grignon, C. (1992) Cloning and expression in yeast of a plant potassium ion transport system. Science 256, 663–665.
[16] Schachtmann, D., Schroeder, J.I., Lucas, W.J., Anderson, J.A. and Gaber, R.F. (1992) Expression of an inward-rectifying potassium channel by the *Arabidopsis KAT1* cDNA. Science 258, 1654–1658.
[17] Bertl, A., Ramos, J., Ludwig, J., Lichtenberg-Frate, H., Reid, J., Bihler, H., Calero, F., Martinez, P. and Ljungdahl, P.O. (2003) Characterization of potassium transport in wild-type and isogenic yeast strains carrying all combinations of *trk1*, *trk2* and *tok1* null mutations. Mol. Microbiol. 47, 767–780.
[18] Madrid, R., Gomez, M.J., Ramos, J. and Rodriguez-Navarro, A. (1998) Ectopic potassium uptake in *trk1 trk2* mutants of *Saccharomyces cerevisiae* correlates with a highly hyperpolarized membrane potential. J. Biol. Chem. 273, 14838–14844.
[19] Dart, C., Leyland, M.L., Barrett-Jolley, R., Shelton, P.A., Spencer, P.J., Conley, E.C., Sutcliffe, M.J. and Stanfield, P.R. (1998) The dependence of Ag^+ block of a potassium channel, murine Kir2.1, on a cysteine residue in the selectivity filter. J. Physiol. 511, 15–24.
[20] Schram, G., Pourrie, M., Wang, Z., White, M. and Nattel, S. (2003) Barium block of Kir2 and human cardiac inward rectifier currents: evidence for subunit-heteromeric contribution to native currents. Cardiovasc. Res. 59, 328–338.
[21] Thompson, G.A., Leyland, M.L., Ashmole, I., Sutcliffe, M.J. and Stanfield, P.R. (2000) Residues be-yond the selectivity filter of the

K^+ channel Kir2.1 regulate permeation and block by external Rb^+ and Cs^+. J. Physiol. 526, 231–240.
[22] Rodriguez-Navarro, A. and Ramos, J. (1984) Dual system for potassium transport in *Saccharomyces cerevisiae*. J. Bacteriol. 159, 940–945.
[23] Cormack, B.P., Valdivia, R.H. and Falkow, S. (1996) FACS-optimized mutants of the green fluorescent protein (GFP). Gene 173, 33–38.
[24] Sambrook, J., Fritsch, E.F. and Maniatis, J. (1989) Molecular Cloning: A Laboratory Manual, second ed, Cold Spring Harbor Laboratory Press, New York.
[25] Rothstein, R. (1991) Targeting, disruption, replacement, and allele rescue: integrative DNA transformation in yeast. Methods Enzymol. 194, 281–301.
[26] Doheny, K.F., Sorger, P.K., Hyman, A.A., Tugendreich, S., Spencer, F. and Hieter, P. (1993) Identification of essential components of the *S. cerevisiae* kinetochore. Cell 73, 761–774.
[27] Plath, K., Wilkinson, B.M., Stirling, C.J. and Rapoport, T.A. (2004) Interactions between Sec complex and prepro-alpha-factor during posttranslational protein transport into the endoplasmic reticulum. Mol. Biol. Cell. 15, 1–10.
[28] Campbell, R.E., Tour, O., Palmer, A.E., Steinbach, P.A., Baird, G.S., Zacharias, D.A. and Tsien, R.Y. (2002) A monomeric red fluorescent protein. Proc. Natl. Acad. Sci. USA 99, 7877–7882.
[29] Gomord, V., Denmat, L.A., Fitchette-Laine, A.C., Satiat-Jeunemaitre, B., Hawes, C. and Faye, L. (1997) The C-terminal HDEL sequence is sufficient for retention of secretory proteins in the endoplasmic reticulum (ER) but promotes vacuolar targeting of proteins that escape the ER. Plant J. 11, 313–325.
[30] Silve, S., Volland, C., Garnier, C., Jund, R., Chevallier, M.R. and Haguenauer-Tsapis, R. (1991) Membrane insertion of uracil permease, a polytopic yeast plasma membrane protein. Mol. Cell. Biol. 11, 1114–1124.
[31] Maresova, L., Sychrova, H. Physiological characterization of *Saccharomyces cerevisiae* kha1 deletion mutants. Mol. Microbiol., in press.
[32] Kolacna, L., Zimmermannova, O., Schwarzer, S., Ludwig, J., Lichtenberg-Frate, H., Sychrova, H. Phenotypic analysis of the mKir2.1 channel activity in potassium efflux deficient *Saccharomyces cerevisiae* strains. IJBCB, submitted for publication.
[33] Bichet, D., Lin, Y.F., Ibarra, C.A., Huang, C.S., Yi, B.A., Jan, Y.N. and Jan, L.Y. (2004) Evolving potassium channels by means of yeast selection reveals structural elements important for selectivity. Proc. Natl. Acad. Sci. USA 101, 4441–4446.
[34] Wright, M.B., Ramos, J., Gomez, M.J., Moulder, K., Scherrer, M., Munson, G. and Gaber, R.F. (1997) Potassium transport by amino acid permeases in *Saccharomyces cerevisiae*. J. Biol. Chem. 272, 13647–13652.
[35] Roberts, S.K., Fischer, M., Dixon, G.K. and Sanders, D. (1999) Divalent cation block of inward currents and low-affinity K^+ uptake in *Saccharomyces cerevisiae*. J. Bacteriol. 181, 291–297.
[36] Bihler, H., Slayman, C.L. and Bertl, A. (2002) Low-affinity potassium uptake by *Saccharomyces cerevisiae* is mediated by NSC1, a calcium-blocked non-specific cation channel. Biochim. Biophys. Acta 1558, 109–118.
[37] Du, Y., Ferro-Novick, S. and Novick, P. (2004) Dynamics and inheritance of the endoplasmic reticulum. J. Cell. Sci. 117, 2871–2878.
[38] Block-Alper, L., Webster, P., Zhou, X., Supekova, L., Wong, W.H., Schultz, P.G. and Meyer, D.I. (2002) IN02, a positive regulator of lipid biosynthesis, is essential for the formation of inducible membranes in yeast. Mol. Biol. Cell. 13, 40–51.
[39] Sagt, C.M., Muller, W.H., van der Heide, L., Boonstra, J., Verkleij, A.J. and Verrips, C.T. (2002) Impaired cutinase secretion in *Saccharomyces cerevisiae* induces irregular endoplasmic reticulum (ER) membrane proliferation, oxidative stress, and ER-associated degradation. Appl. Environ. Microbiol. 68, 2155–2160.
[40] Mercier, R.W., Rabinowitz, N.M., Ali, R., Gaxiola, R.A. and Berkowitz, G.A. (2004) Yeast hygromycin sensitivity as a functional assay of cyclic nucleotide gated cation channels. Plant Physiol. Biochem. 42, 529–536.
[41] Haro, R. and Rodriguez-Navarro, A. (2002) Molecular analysis of the mechanism of potassium uptake through the TRK1 transporter of *Saccharomyces cerevisiae*. Biochim. Biophys. Acta 1564, 114–122.